

Nonlinear Elimination Preconditioned Space-Time Solution Algorithms for Hyperbolic Problems

Chang-Wen Liang^[0009-0003-2723-3189] and Feng-Nan Hwang^[0000-0002-2012-3257]

1 Introduction

Fully coupled space-time methods for time-dependent partial differential equations (PDEs) have recently gained popularity for parallelization in the temporal domain, thanks to increased computing power [2, 7]. These algorithms require solving large, spatial, nonlinear systems simultaneously, necessitating a robust and efficient nonlinear solver as a critical component of the entire solution algorithm. This paper studies some nonlinear preconditioned Newton algorithms for the space-time formulation of hyperbolic equations with shocks. In this case, the classical inexact Newton method with backtracking (INB) suffers from long stagnation due to local strong nonlinearity. Nonlinear preconditioning, such as nonlinear elimination, has been shown to improve the robustness of INB for many types of PDEs [3, 4, 5, 6] but does not work well for hyperbolic PDEs. To address this, we propose a new variant of nonlinear elimination preconditioners designed specifically for hyperbolic PDEs, considering their characteristics to overcome the associated difficulties. We conduct a comparative study of inexact Newton algorithms in conjunction with left and right nonlinear elimination preconditioning, namely INB-ANE [3] and NEPIN [5], respectively, to validate our proposal.

Let us begin by considering a model problem, the 1D Burgers' equation in the conservation form,

$$\frac{\partial u(x, t)}{\partial t} + \frac{\partial \left(\frac{1}{2} u^2(x, t) \right)}{\partial x} = 0,$$

Chang-Wen Liang
Department of Mathematics, National Central University, Taoyuan City 320317, Taiwan,

Feng-Nan Hwang
Department of Mathematics, National Central University, Taoyuan City 320317, Taiwan, e-mail:
hwangf@math.ncu.edu.tw

on a space-time domain $\Omega = [a, b] \times [0, T]$, with some proper initial and boundary conditions if needed. Let

$$U = [u_1^1, u_2^1, \dots, u_n^1, u_1^j, \dots, u_i^j, \dots, u_n^j, \dots, u_1^m, u_2^m, \dots, u_n^m]^T$$

be approximate solutions on each grid point, i.e., $u_i^j \approx u(x_i, t_j)$, $x_i = x_0 + i\Delta x$ with $\Delta x = (b - a)/n$ and $t_j = t_0 + j\Delta t$, with $\Delta t = T/m$, where $1 \leq i \leq n$ and $1 \leq j \leq m$, respectively. Here, n and m are the spatial and temporal grid numbers. We use the local Lax-Friedrichs method [2] for spatial discretization and forward Euler's method for temporal discretization to derive a full coupled space-time large, sparse, nonlinear system of equations, $F(U) = 0$, where $F = [F_1^1, F_2^2, \dots, F_n^1, F_1^j, \dots, F_i^j, \dots, F_n^j, \dots, F_n^m]^T$. Here,

$$\begin{aligned} F_i^{j+1} = & u_i^{j+1} - \left(u_{i-1}^j + |u_i^j| + |u_{i-1}^j| \right) \frac{\Delta t}{4\Delta x} u_{i-1}^j - \left[1 - \left(|u_{i+1}^j| + 2|u_i^j| + |u_{i-1}^j| \right) \frac{\Delta t}{4\Delta x} \right] u_i^j \\ & + \left(u_{i+1}^j - |u_{i+1}^j| - |u_i^j| \right) \frac{\Delta t}{4\Delta x} u_{i+1}^j \end{aligned}$$

We focus on studying the performance of INB, INB-NE, and NEPIN on two test cases of Burgers' equations [1]: (1) Single shock: Defined on $[0, 1] \times [0, 1]$ with the initial and boundary conditions

$$u(x, t) = \begin{cases} 0.5 & \text{if } t = 0, \\ 1 & \text{if } x = 0. \end{cases}$$

(2) Double shock: Defined on $[0, 2] \times [0, 1]$ with the initial and boundary conditions

$$u(x, t) = \begin{cases} 1.5 & \text{if } t = 0, x \leq 0.5 \\ 0.5 & \text{if } t = 0, x > 0.5 \\ 2.5 & \text{if } x = 0. \end{cases}$$

Fig. 1 shows the numerical solution plots for each case.

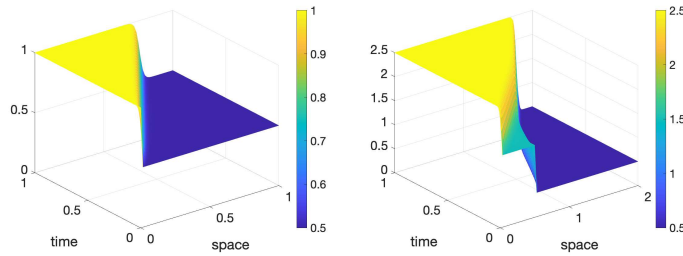


Fig. 1: Numerical solutions for single (left) and double shock (right) problems on the 64×128 grid.

2 Residual-based elimination challenges and remedies in hyperbolic PDEs

We outline the key steps in NEPIN and INB-ANE, which are listed in Table 1. The notations used in the algorithm are defined as follows. Let $S = \{1, 2, \dots, mn\}$ be an index set (one integer for each unknown and each nonlinear function), where $mn = m \times n$. Suppose the index set can be partitioned into two subsets, i.e., $S_b \cup S_g = S$. The subset S_b corresponds to the components causing the failure of Newton's convergence. $R_b : R^{mn} \rightarrow V_b$ is a restriction operator for the bad components, where $V_b = \{v | v = (v_1, \dots, v_{mn})^T \in R^{mn}, v_k = 0 \text{ if } k \in S_g\}$. Similarly, the restriction operator for good components, R_g , is defined as a mapping from R^{mn} to V_b^c . $F_b : R^{mn} \rightarrow V$ as $F_b = R_b F$ is a nonlinear subspace function. G_L and G_R are referred to as the left and right preconditioning operators, respectively.

We point out the similarities and differences between the two methods. NEPIN and INB-ANE solve a subspace problem in step 1 and place Z into the Jacobian matrix. However, step 2 uses a different residual vector on the right-hand side when solving the inexact Newton direction using the Jacobian system. Additionally, NEPIN updates the approximate solution in step 3, similar to the modified Euler method for the first-order initial value problems, by starting from the original solution and updating it using the new direction. In contrast, for INB-ANE, the approximate solution update is treated as a prediction correction, where it updates from the new solution Z and computes the new direction based on Z .

NEPIN (left preconditioner)	INB-ANE (right preconditioner)
For a given partition $U = [U_b, U_g]$,	For a given partition, $U = [U_b, U_g]$
1. Compute $Z = [U_b - T_b, U_g]$ by solving the subspace problem	1. Compute $Z = G_R(U) = [T_b, U_g]$ by solving the subspace problem,
$F_b(U_b - T_b, U_g) = 0$ for T_b .	$F_b(T_b, U_g) = 0$ for T_b .
Form global residual vector	
$g = G_L(F(U)) = \begin{bmatrix} J_b(Z)T_b \\ F_g(U) \end{bmatrix}$,	
where $J_b(Z) = F'_b(Z)$.	
2. Find the inexact Newton direction d by solving	2. Find the inexact Newton direction d by solving
$J(Z)d = -g$, where $J(Z) = F'(Z)$.	$J(Z)d = -F(Z)$, where $J(Z) = F'(Z)$.
3. Update the new approximate solution	3. Update the new approximate solution
$U = U + \lambda d$.	$U = Z + \lambda d$.

Table 1: Step-by-step comparison of NEPIN and INB-ANE.

Next, Table 2 compares nonlinear iteration counts for INB and INB-ANE with various grid sizes and three initial vectors. The results show that nonlinear elimination preconditioning can reduce the number of global Newton iterations; however, the

grid size still affects iteration counts, which is not observed for other types of PDEs. Here, the algebraic-based elimination strategy is used to determine the subset of S for the bad components S_b . That is for all $1 \leq i \leq mn$ such that $|F_i(U)| > \rho \|F(U)\|_2$, where $0 < \rho < 1$ is a pre-chosen constant, e.g., $\rho = \frac{1}{mn}$.

$n \times m$	64×128	128×256	256×512	512×1024
A zero initial vector				
INB	28	59	129	283
INB-ANE	24	49	105	231
A constant initial vector with boundary condition value				
INB	14	31	46	211
INB-ANE	7	18	27	69
A constant initial vector with initial condition value				
INB	7	13	30	49
INB-ANE	6	10	20	26

Table 2: Single shock case. A comparison of several Newton iterations with different grid sizes. Three initial guess vectors are used for both cases.

Through extensive numerical experiments, plotting point-wise residuals, errors, and components to be eliminated, as well as the residual norm history, we identified issues with the residual-based elimination strategy. A small residual does not always indicate a small error, which can lead to an inaccurate identification of bad components. For example, in the single shock problem with a zero vector as the initial guess, Fig. 2 shows weak correlation between residuals and errors, suggesting the subspace correction step does not effectively reduce the impact of bad components on Newton's convergence. In addition, Fig. 3 (a) illustrates that domain

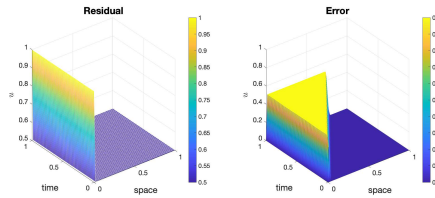


Fig. 2: Single shock problem. A comparison of the point-wise residual and point-wise error when a zero initial guess is used.

dependence for hyperbolic PDEs differs significantly from that of elliptic ones. In elliptic problems, impact is highest near the center of a circular domain. In contrast, for hyperbolic problems, all points within the triangle affect the value at the point of interest. Therefore, a subdomain with a hole, as shown in Fig. 3 (b), leads to lost

information and unphysical discontinuities near the hole. These factors are believed to cause the ineffectiveness of the original nonlinear elimination preconditioning for hyperbolic problems.

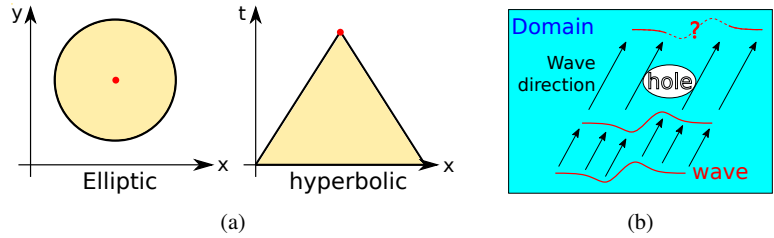


Fig. 3: (a) Difference in the domain of dependence for elliptic and hyperbolic PDEs. (b) Information loss in a subdomain with a central void.

We use a coarse-grid correction technique from multigrid methods to address the issue where a small residual does not indicate a small error. By solving the nonlinear problem on a coarse grid and using this solution as an initial guess for the fine grid, we eliminate low-frequency errors. For example, in the discrete Burgers' equation with forward and backward Euler methods in time and space, respectively, $F(U) = \frac{u_j^{n+1} - u_j^n}{\Delta t} + \frac{\frac{1}{2}(u_j^n)^2 - \frac{1}{2}(u_{j-1}^n)^2}{\Delta x}$, using a zero initial guess yields zero residuals everywhere but significant error, as shown in the top of Fig. 4. With the coarse-grid correction (bottom of Fig. 4), we see noticeable errors and nonzero residuals, effectively identifying the components to be eliminated. Secondly, we use the mor-

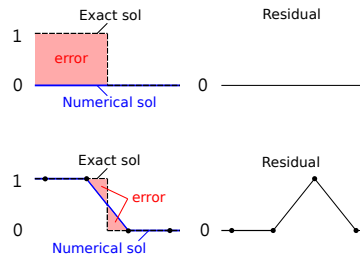


Fig. 4: The relation between residual and error components for two cases, if a zero guess or an interpolated coarse solution is used as an initial guess.

phological closing operation from image processing to remove small holes in the subdomain (see Fig.5 (a)). This operation involves dilation followed by erosion using a disk structuring element. Fig. 5 (b) shows the original domain and the result after applying this operation in the INB-ANE algorithm, clearly demonstrating the removal of holes, gaps, and isolated islands.

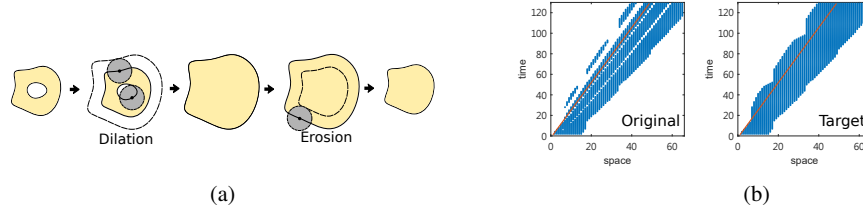


Fig. 5: (a) The morphological closing. (b) The original subdomain and the one obtained after the morphological closing operation.

3 Numerical results

Table 3 summarizes the comparative numerical results of different algorithms with different grid sizes, from $(n, m) = (64, 128)$ to $(512, 1024)$ in single and double shock problems. The algorithms include traditional INB-ANE, INB-ANE with hole fill-in (INB-ANE+HF), NEPIN, and NEPIN with hole fill-in (NEPIN+HF), with the hole fill-in method using a disk structuring element of radius n . The table shows that global Newton iterations increase rapidly with grid refinement in traditional INB-ANE, especially for double shocks, where iterations quadruple from 256×512 to 512×1024 . To address this, we applied a morphological closing operation to improve the identification of bad components, incorporating it into INB-ANE and NEPIN. Hole fill-in notably reduces global Newton iterations in INB-ANE to 3.7% at 512×1024 . However, computational costs also depend on subspace iterations and selection size. As the grid size increases, the bad component rate decreases by about 60% from 64×128 to 512×1024 . NEPIN+HF shows better performance than INB-ANE+HF, especially in computing time.

Fig. 6 shows the evolution of bad components in the space-time domain for the single shock case over the first four iterations of INB-ANE and NEPIN with $(n, m) = (256, 512)$. The blue regions indicate bad components, and the white regions represent good components. The red line marks the exact shock position. Initially, both methods reduce to classical Newton, exhibiting identical residual values and subspace domain sizes. However, by the second global iteration, a significant difference emerges: NEPIN selects fewer bad components along the shock line than INB-ANE, leading to reduced average overhead in each subspace problem. To understand why INB-ANE requires more bad components, refer to the left side of Fig. 7, which shows the distribution of bad elements in the space-time domain after the first global iteration. Along the $t = 0.5$ line, bad components are located between $x = 0.3$ and $x = 0.6$. The middle and right sides of the figure display the intermediate solution (top) and pointwise residual (bottom) for both INB-ANE and NEPIN at $t = 0.5$. The discontinuity in the INB-ANE solution at the interface between bad and good components leads to peaks in the pointwise residuals, influencing the selection of bad components in the next iteration. In contrast, NEPIN accurately captures the shock location, enhancing the convergence of Newton's methods.

		Single shock case			
		64×128	128×256	256×512	512×1024
INB-ANE	Global Newton steps (gmres)	4 (16)	5 (20)	14 (56)	22 (88)
	Subspace Newton steps (ER)	7 (0.21)	10 (0.17)	32 (0.12)	66 (0.08)
	Total compute time (s)	0.38	0.58	4.02	29.51
INB-ANE + HF	Global Newton steps (gmres)	4 (16)	4 (16)	4 (16)	5 (20)
	Subspace Newton steps (ER)	6 (0.38)	7 (0.28)	24 (0.40)	59 (0.39)
	Total compute time (s)	0.42	0.50	2.07	16.49
NEPIN	Global Newton steps (gmres)	5 (20)	5 (20)	7 (26)	9 (34)
	Subspace Newton steps (ER)	7(0.21)	10(0.17)	19(0.14)	31(0.11)
	Total compute time (s)	0.37	0.57	2.29	12.60
NEPIN + HF	Global Newton steps (gmres)	4 (16)	5 (20)	5 (20)	7 (26)
	Subspace Newton steps (ER)	6 (0.38)	8(0.26)	21 (0.23)	43 (0.20)
	Total compute time (s)	0.36	0.58	2.08	13.78
		Double shock case			
		64×128	128×256	256×512	512×1024
INB-ANE	Global Newton steps (gmres)	7 (27)	11 (43)	42 (167)	163 (651)
	Subspace Newton steps (ER)	17(0.17)	45 (0.11)	113 (0.09)	484 (0.07)
	Total compute time (s)	0.45	1.07	12.14	221.35
INB-ANE + HF	Global Newton steps (gmres)	4 (16)	5 (20)	5 (20)	6 (24)
	Subspace Newton steps (ER)	15 (0.35)	40 (0.38)	63 (0.37)	328 (0.32)
	Total compute time (s)	0.47	1.01	4.46	81.74
NEPIN	Global Newton steps (gmres)	6(24)	8(29)	F	F
	Subspace Newton steps (ER)	16(0.19)	41 (0.13)	F	F
	Total compute time (s)	0.48	1.09	F	F
NEPIN + HF	Global Newton steps (gmres)	5(20)	5 (20)	6 (23)	7 (27)
	Subspace Newton steps (ER)	16 (0.34)	37 (0.31)	56 (0.29)	312 (0.28)
	Total compute time (s)	0.48	0.94	4.17	78.57

Table 3: The single shock and double shocks case with different algorithms. We set stopping conditions for global Newton iterations relative $tol = 10^{-8}$, for local Newton iterations relative $tol = 10^{-3}$, GMRES iterations $tol = 10^{-6}$. “F” indicates the failure of convergence. “ER” is the average rate of eliminated bad component per subspace iteration.

4 Conclusions

We compared the performance of two nonlinear preconditioned iterative algorithms, INB-ANE and NEPIN, using Riemann problems for the inviscid Burgers’ equation. A coarse-grid correction and morphological closing operation are applied to more accurately identify regions of strong local nonlinearity. The results demonstrated that NEPIN, combined with these two new techniques for hyperbolic PDEs with shocks, outperformed INB-ANE in identifying the correct shock location and introducing less interface pollution. Additionally, the number of Newton iterations required for NEPIN to converge was almost independent of the time step and mesh size.

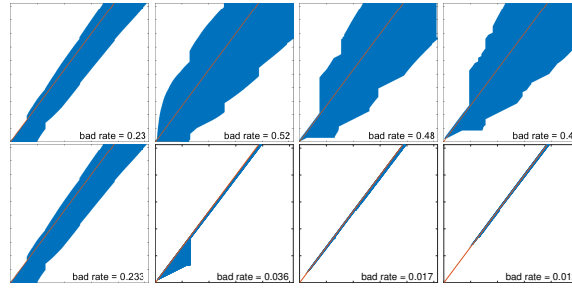


Fig. 6: Distribution evolution of bad components: INB-ANE (first row) and NEPIN (second row). First four global Newton iterations. Bad rate is the percentage of components to be eliminated relative to the total number of components.

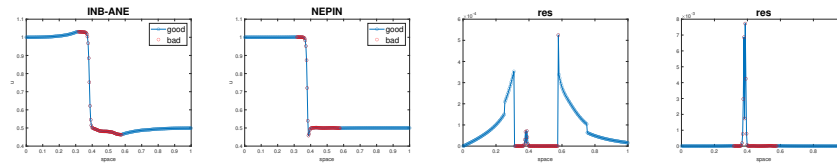


Fig. 7: The one-step global solution, and the global residual for the single shock case at $t = 0.5$ with a grid of 256×512 .

References

1. H. De Sterck, T.A. Manteuffel, S.F. McCormick, and L. Olson. Numerical conservation properties of H(div)-conforming least-squares finite element methods for the Burgers equation. *SIAM J. Sci. Comput.*, 26:1573–1597, 2005.
2. A.J. Howse, H. De Sterck, R.D. Falgout, S. MacLachlan, and J. Schroder. Parallel-in-time multi-grid with adaptive spatial coarsening for the linear advection and inviscid Burgers equations. *SIAM J. Sci. Comput.*, 41(1):A538–A565, 2019.
3. F.-N. Hwang, Y.-C. Su, and X.-C. Cai. A parallel adaptive nonlinear elimination preconditioned inexact Newton method for transonic full potential equation. *Comput. Fluids*, 110:96–107, 2015.
4. L. Liu, W. Gao, Han Yu, and D.E. Keyes. Overlapping multiplicative Schwarz preconditioning for linear and nonlinear systems. *J. Comput. Phys.*, 496:112548, 2024.
5. L. Liu, F.-N. Hwang, L. Luo, X.-C. Cai, and D.E. Keyes. A nonlinear elimination preconditioned inexact Newton algorithm. *SIAM J. Sci. Comput.*, 44:A1579–A1605, 2022.
6. L. Luo, W.-S. Shiu, R. Chen, and X.-C. Cai. A nonlinear elimination preconditioned inexact Newton method for blood flow problems in human artery with stenosis. *J. Comput. Phys.*, 399:108926, 2019.
7. H. Yang and F.-N. Hwang. A nonlinear elimination preconditioner for fully coupled space-time solution algorithm with applications to high-Rayleigh number thermal convective flow problems. *Comput. Phys. Commun.*, 26:749–767, 2019.